

Aerodynamic Analysis of Turboprop Engine Air Intake

P. Chudý, K. Fiřakovský, J. Friedl

The objective of this paper is to present CFD computation of a LET L-410 engine nacelle equipped with a Walter M-601E turboprop engine. The main purpose is to estimate the air intake fluid characteristics of different air intake geometries. The results of these computations are part of an optimisation process focused on increasing the performance and reducing the losses in the 'engine – nacelle' system. A problem with flow separation in the input section was observed. This project is supported by Ministry of Industry and Trade of the Czech Republic.

Keywords: aerodynamic, CFD, turboprop engine, air intake.

1 Introduction

Turboprop engines are widely used in a category of commuter aeroplanes. The main considerations for correct function of a turboprop engine, from the aerodynamic point of view, are losses in the air intake section and drag of the engine nacelle. As a basis for further consideration we chose an L-410 UVP-E aeroplane equipped with twin Walter M-601E engines and Avia V-510 propellers. The general goals were to analyse the flow field around its engine nacelle and in whole intake section using the CFD method, and to provide set of basic aerodynamic characteristics with certain variations of air intake and nacelle geometry.

The CFD package CFX 5.5 was used to model this complex problem. The Finite Volume Method was implemented for numerical solution of the Navier-Stokes equation. It the choice of different models for turbulence.

A computation run was done at two computers at IAE, a Silicon Graphics Origin 2100 workstation with eight processors running under the Unix platform and a twin-processor PC running under the Windows 2000 platform.

2 Data preparation

2.1 Geometric simplification

One consideration when dealing with such a complex problem is to be as close as possible to the reality. On other hand there are of course certain limits, e.g., when modelling geometric details, allowable solver time, etc. We therefore decided to neglect minor and complicated structural elements in the stilling chamber and in the inlet duct into the axial compressor (rivets, engine mount, blades, etc.)

2.2 Geometry

The geometry of the nacelle and air intake was created from 2D documentation obtained by Letecké závody a.s. The Unigraphics (UG) CAD system was used for digitising the geometric data. Points, curves and surfaces to describe complicated geometric layout. The geometry involves an external part and an internal part. The external parts consist of the nacelle, the torso of the wing with a span of 2 m and appropriate airfoil sections the external part of the exhaust, the propeller hub spinner (see Fig. 1). The internal part consists of the nacelle, featuring the air intake, the stilling



Fig. 1: External part of nacelle geometry

chamber and the engine protection screen, covering a part of an axial compressor inlet duct (see Fig.2). For importing CAD data into the CFX preprocessor an IGES file was created.



Fig. 2: Internal part of nacelle geometry

2.3 Computational domain

For preprocessing, CFX Build was used to prepare data for the solver. The IGES file was imported into preprocessor, where the geometry was reconstructed and a solid for whole computational domain was created. The domain consists of a semi-spherical front part and a cylindrical rear part. As the creation of the solid was successfully performed surface seeds,

the setting of prismatic elements and volume mesh refinement controls were applied at expected areas of main flow changes and a volume mesh was generated. It proved very difficult to set appropriate values of mesh controls due to the geometric complexity of the model. A number of elements in the unstructured hybrid mesh varied up to 1.3 millions. The surface mesh is shown at Fig. 3.

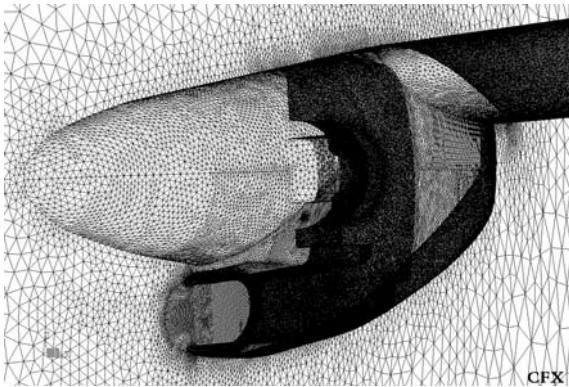


Fig. 3: Surface mesh at nacelle and symmetry plane

2.4 Boundary condition

The task was assumed with one plane of symmetry in order to decrease solution time. The boundary conditions (BC) were chosen as follows. For free stream input into a domain, a velocity-inlet (“Inlet”) was used, an “Outer wall”

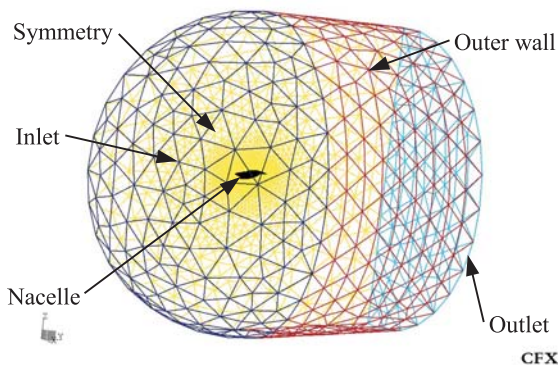


Fig. 4: Global BC

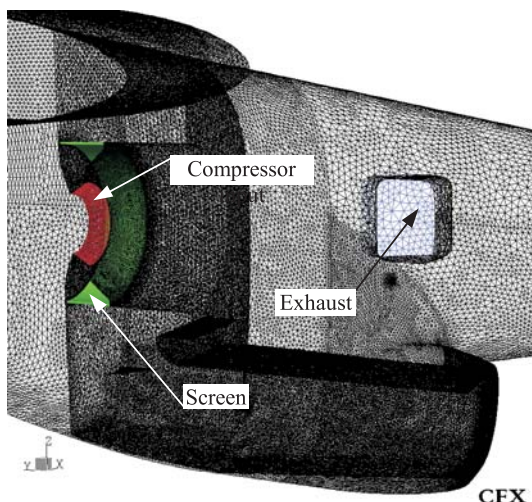


Fig. 5: BC at Nacelle

was defined as a wall with no slip, an “Outlet” was defined as a pressure-outlet from the domain. For the “Nacelle” we used a wall, at the “Compressor input” pressure-outlet was defined (from the domain’s point of view it is in fact output of the flow), influence of “Exhaust” as pressure-inlet (see Fig. 4, 5). A certain pressure loss, computed from the screen geometry [1], was defined at the “Screen” (subdomain) as a linear loss coefficient, according to user’s reference guide [2] (see Fig. 5).

2.5 Monitor surfaces

For the computed case, comparison sets of monitor surfaces were defined to determine the flow characteristics in these sections (see Fig. 6).

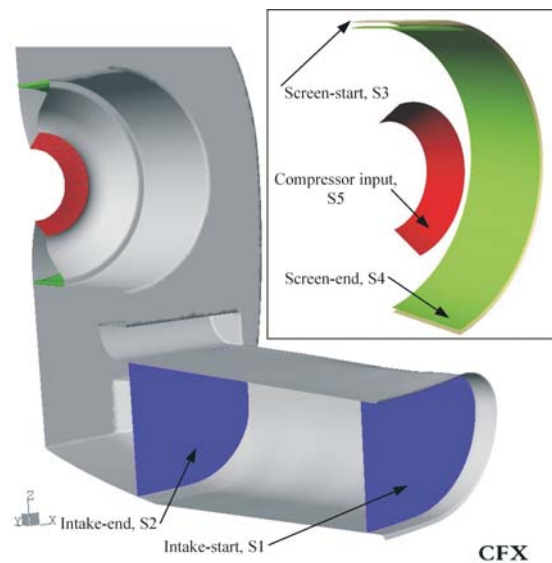


Fig. 6: Monitor surfaces in air intake and detail at stilling chamber

2.6 Flow parameters and solver setting

All computations were done with the following set of parameters. Free stream velocity value $v_f = 250$ kph and the further parameters according to International Standard Atmosphere at the flight altitude $H_p = 1500$ m. The fluid was modelled as incompressible gas due to the relatively low flight speed. The influence of free stream velocity and static pressure defined on the basis of ideal propeller propulsion theory [3, 4], and the propeller stream slip was neglected (this allows a single symmetry plane to be used). A turbulence intensity value 4 % behind the propeller was estimated. All solver runs were realised as parallel on the computers. The tasks were set as an unsteady solution with a small time step, due to complications with convergence during steady runs.

3 Computed cases

3.1 Computation process

The CFX Solver was used for all computations. The solution time for one case varied up to few days. The computation process always has the same scheme. Firstly, in several steps, the mass flow ratio through the engine was “tuned” by setting the of static pressure value at BC “Compressor input” (the mass flow value was given for this work regime of the engine).

Finally the pressure loss at the subdomain “Screen” was set to achieve a drop in total flow pressure through the screen. The allowable differences between the two known and computed values were considered as $\pm 3\%$. Under the computation reached a value for all maximal residuals under $1 \cdot 10^{-4}$ the solution was declared as converged.

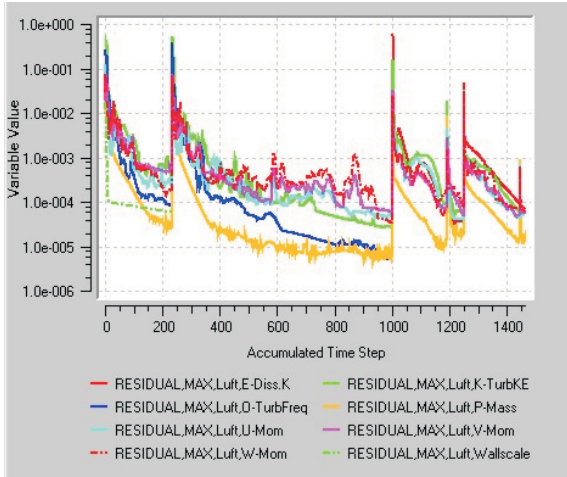


Fig. 7: Typical history of convergence, for original air intake turbulence model k-ε

3.2 Solutions:

The main goal in this project was to provide aerodynamic data for different air intake geometries. Five geometric variations were computed, as follows:

- Original air intake,
- Air intake +10 %,
- Air intake – 10%,
- Air intake with prismatic insert,
- Optimised air intake.

In all cases the k-ε turbulence model was used, except in the Original air intake case where a k-ω SST turbulence model was used.

A shape of the air intake +10 % was determined from the original air intake with the cross section areas increasing by +10 %. Designing the air intake –10 % geometry, we used the same process, and the areas of the cross sections were decreased. The geometry of the air intake with a prismatic insert has a constant area up to a length of 138 mm from the front section, then an expansion of the cross section areas to the original geometry was created. The prismatic length value was determined using laminar and turbulent boundary layer theory simplified for 2 dimensions [5]. The optimised air intake geometry also has a prismatic front part 138 mm in length and an expansion of the cross section areas according to boundary layer theory of flow against back pressure was used [5, 6, 7]. In all cases the total length of the channel was identical. The geometry of the stilling chamber was also identical in all cases (except the optimised case).

4 Results and visualisation

The main flow characteristics were monitored at surfaces S1–S5, and the total pressure losses in the internal sections were determined (see Table 1).

Table 1: Summary of results

Air intake case	Pressure loss channel	Pressure loss stilling chamber	Total pressure loss	Ratio chamber/channel
-	[Pa]	[Pa]	[Pa]	[1]
Original k-ε	158.13	278.02	436.15	1.758
Original k-ω SST	53.77	255.79	309.56	4.757
Insert	63.13	240.23	303.36	3.805
-10 %	49.97	237.02	286.99	4.743
+10 %	45.40	231.08	276.48	5.090
Optimized	127.30	223.53	350.83	1.756

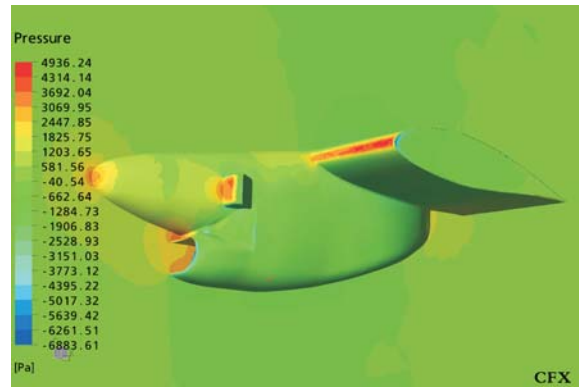


Fig. 8: Contours of static pressure (relative to the reference pressure), original air intake, k-ε turbulence model

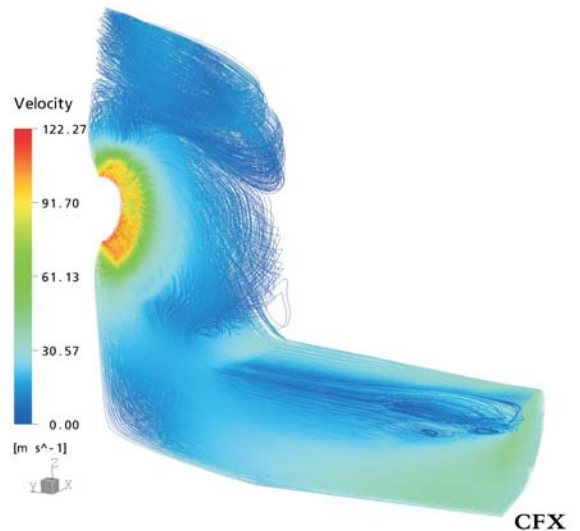


Fig. 9: Streamlines in internal sections, original air intake, k-ε turbulence model

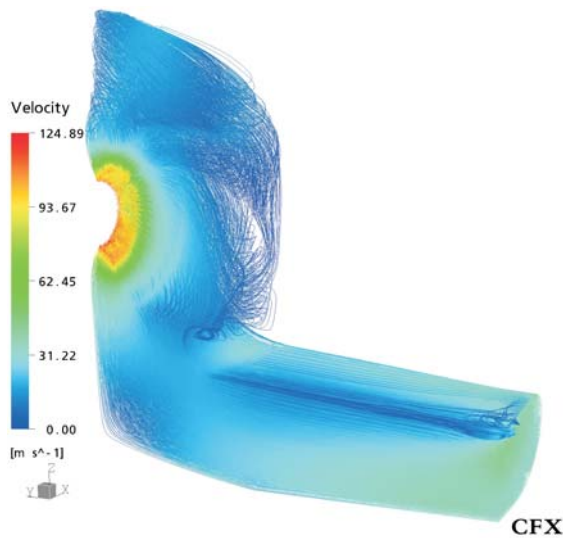


Fig. 10: Streamlines in internal sections, original air intake, $k-\omega$ SST turbulence model

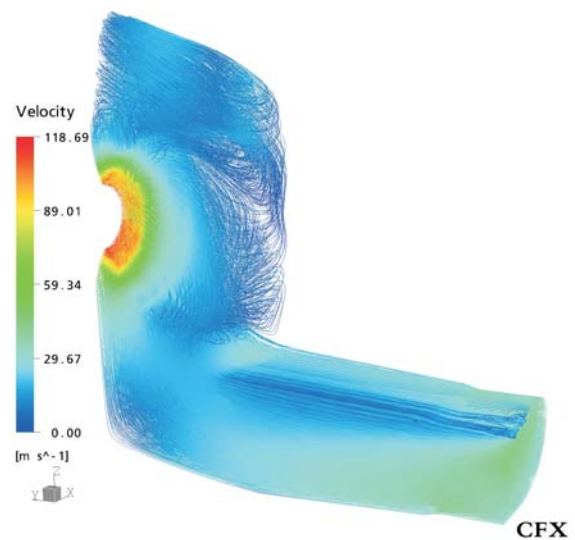


Fig. 13: Streamlines in internal sections, air intake with insert, $k-\omega$ turbulence model

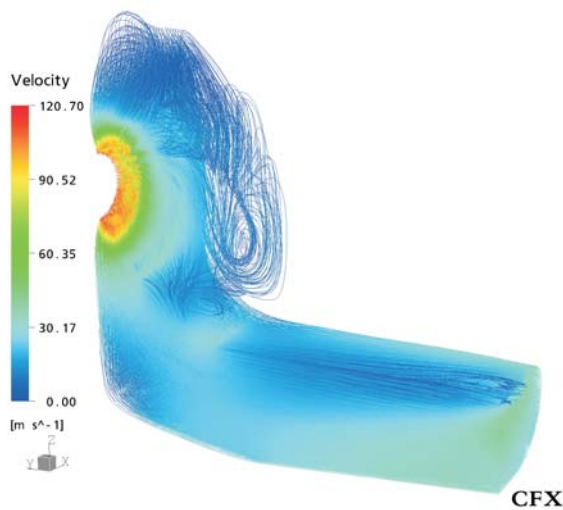


Fig. 11: Streamlines in internal sections, air intake +10%, $k-\omega$ turbulence model

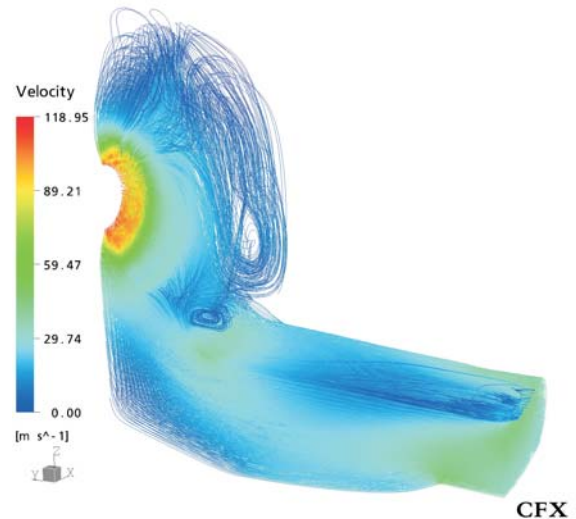


Fig. 14: Streamlines in internal sections, air intake with insert, $k-\omega$ turbulence model

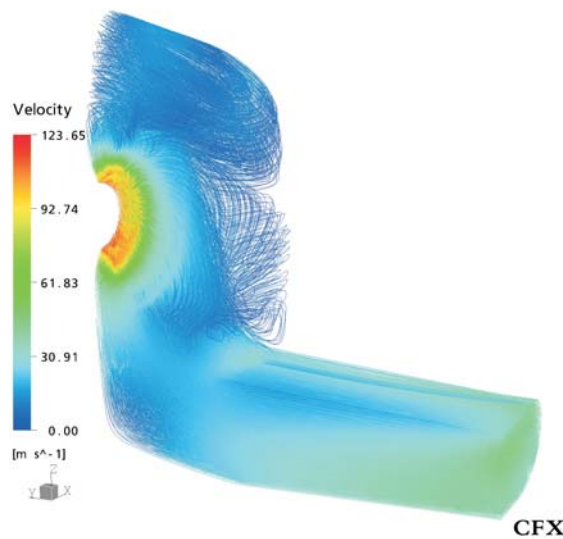


Fig. 12: Streamlines in internal sections, air intake -10%, $k-\omega$ turbulence model

5 Comparison with experiment

The experiment was performed by Walter a.s. in a static test room for engines [8]. The experimental set-up was relatively simple, and the main goal was to confirm or refuse the appearance of a certain separation area in the original intake geometry. For analysis we used the method of visualisation of flow by cotton fibres, which were stuck to the upper side of the channel in a 50×50 mm grid. A small digital industrial camera was used to record the measurements. It was mounted on the operating platform. Due to the impossibility of seeing through the nacelle structure, the bottom part of channel was replaced by appropriately blended acrylic glass, and the external structure part was cut out. The experiment confirmed the appearance of a certain separation area during all regimes from free wheel up to maximum thrust. For illustration purposes, the case with maximum thrust in Fig. 15 shows separation and recirculating zones with large movement of the fibres (unfocused).

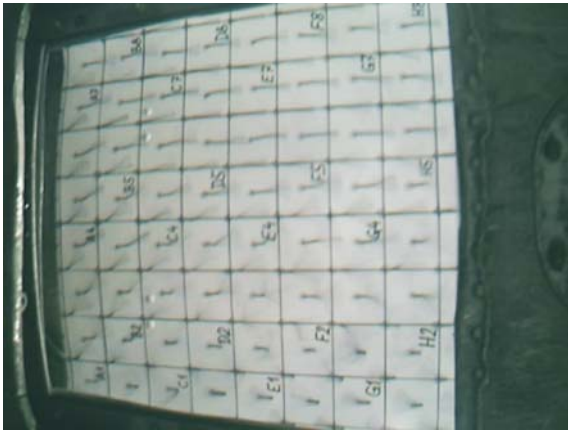


Fig. 15: Flow visualisation in channel

6 Discussion of results, and conclusions

This work successfully shows a CFD analysis of different turboprop air intake geometries, although the process of creating computer models was extremely time consuming. Some conclusions from the computed results and experiment can be presented, but for a detailed analysis more sophisticated experiment at work is needed (pressure taps, measurement of intensity turbulence, etc.) The first computed case of the original air intake geometry with the $k-\epsilon$ turbulence model has a wide flow separation area, beginning of the channel, which results in high total pressure loss. The second analysis, the case of the original air intake with turbulence model $k-\omega$ SST, shows a smaller separation area, and the total pressure loss is three times smaller than in the previous case. Channel geometry variants modified by increments of +10 % and -10 % show a relatively small separation and also a small total pressure loss value. The case of air intake with a prismatic insert has less total pressure loss than the original $k-\omega$ case, but the advantages of this geometric modification are controversial. Optimised geometry has incomparable results for major geometry changes in the channel, bottom part of the stilling chamber and also in the external shape of nacelle. All cases show that an extremely high pressure drop has occurred in the stilling

chamber, so in order to further decrease the pressure drop in the whole air intake the complete geometry of the channel and stilling chamber must be modelled as a simple part and modified.

This project successfully shows that even quite complex configurations can be simulated via CFD codes, but comparison with experimental values is essential.

References

- [1] Rae W. H., Pope A.: *Low-Speed Wind Tunnel Testing*. John Wiley & Sons, N. Y., 1984.
- [2] CFX User's manuals
- [3] Alexandrov V. L.: *Letecké vrtule*. SNTL, Praha, 1954.
- [4] Švéda J.: *Teorie vrtulí a vrtulníků*. Skripta VA Brno, 1962.
- [5] Schlichting H.: *Boundary Layers Theory*. McGraw-Hill, 1979.
- [6] Fiřakovský K.: "Graficko-analytická metoda riešenia TMV". Sborník VA Brno, řada B (1966), č. 6.
- [7] Fiřakovský K., Pavelek M.: "2D TMV s vlivem tlakového spádu". Stát. úkol zákl. výzkumu III-4-2/01-2 zpráva za rok 81/82, 1982.
- [8] Sláčík S.: "Optimalizace zástavby turbovrtulového motoru". Výzkumná zpráva. Walter a.s., Praha, 2003.

Ing. Peter Chudý
phone: +420 541 143 370
e-mail: chudy@lu.fme.vutbr.cz

Prof. Ing Karol Fiřakovský, CSc.
phone: +420 541 142 235
fax: +420 541 142 879
e-mail: fil@lu.fme.vutbr.cz

Ing. Jan Friedl
phone: +420 541 143 470
e-mail: friedl@lu.fme.vutbr.cz

Institute of Aerospace Engineering
Brno University of Technology
Technická 2
616 69 Brno, Czech Republic